Quantitative Molecular Sensing Using DNA Origami

Spring 2016

Submitted by: Lavanya Easwaran
Faculty Advisor: Dr. Carlos Castro, Department of Mechanical and Aerospace Engineering
Graduate mentor: Jenny Le, PhD candidate, Interdisciplinary Biophysics Graduate Program
Thesis Committee: Dr. Carlos Castro, Dr. Nicholas Brunelli, and Dr. Madhura Pradhan

Abstract

Type I diabetes is considered a worldwide epidemic because its incidence is exponentially increasing. Current treatment of the disease requires blood glucose monitoring and intake of insulin. While there have been many medical advances in devices that monitor glucose and deliver insulin, these treatments can still lead to complications, including but not limited to debilitating hypoglycemia, neuropathy, and death, if not followed properly. To eliminate these complications, there is a need to create a novel approach for continuous and automated glucose monitoring and insulin delivery. This project seeks to address this challenge by creating a DNA nanostructure that can sense changes in the concentration of a target biomolecule. The long-term goal is to use this DNA nanostructure to detect a glucose-protein complex. The nanostructure comprises a DNA hinge with aptamers (short DNA strands with sequences that bind to a specific protein). Initial development and optimization experiments will target the protein thrombin for simplicity and easy availability. We use transmission electron microscopy (TEM) to measure the equilibrium changes in conformation of the hinge upon contact with thrombin. We initially explored two conformations of the hinge: one that opens when it comes into contact with thrombin and another that closes. Preliminary TEM results have shown that the closed structure is more efficient for detection. In the future, we plan to conduct fluorescence experiments to further optimize the protein sensor and measure real-time response. These experiments will lay the foundation for a viable long-term glucose sensor; the sensor can then be paired with a molecular release mechanism to deliver insulin. Ultimately, this type of device could serve as an automated monitoring and delivery system that would make diseases such as diabetes more manageable and eliminate many of the complications that arise from current treatments.

Acknowledgments

I would like to acknowledge and express my sincerest gratitude to my advisor, Dr. Carlos Castro for his assistance with the foundation and development of project as well as his interest in my continued improvement in lab technique. I also would like to thank him for all his support and teaching during the course and submission of this thesis.

I would also like to acknowledge and thank my graduate mentor, Jenny Le, for supporting me with the data collection for this project as well as her never-ending assistance in completing the protocols, figures, and writing for this thesis.

I would also like to thank Dr. Robert Siston for his assistance in the development of my oral research presentation and his support of undergraduate research. Additionally, I would like to thank Dr. Nicholas Brunelli and Dr. Madhura Pradhan for their willingness to serve on my committee and advise me in the completion of this thesis

I would like to acknowledge and thank Molly Mollica and Patrick Halley for their assistance with the writing of this thesis and their willingness to assist with the creation of the figures. I would like to thank Alex Marras for his assistance with modifying the hinge design. Finally, I would like to thank all of the members of the Nanoengineering Biodesign Laboratory for this support and wonderful personalities.

Table of Contents

Table of Figures and Tables

Chapter 1: Introduction

1.1 Type 1 and Type 2 Diabetes

Diabetes Mellitus is a group of metabolic diseases that are characterized by excess glucose in the bloodstream. The presence of the excess glucose is due to the deficiencies in insulin secretion, insulin action or both. The vast majority of cases of diabetes fall into two categories: type 1 diabetes and type 2 diabetes. The cause of Type 2 diabetes is both a resistance to insulin action and a deficiency in insulin secretion. Also known as immune-mediated diabetes, Type 1 diabetes is caused by the absence of insulin secretion. Type 1 diabetes (T1D) is the motivation for this study. This is because it is the more severe form of diabetes and because large epidemiologic studies have shown the incidence of T1D is increasing by 2-5% worldwide with a prevalence of 1 in 300 in the US by 18 years of age. Currently, T1D accounts for 5-10% of total cases of diabetes worldwide and continues to be the most common type of diabetes in children and adolescents[1]. The immunological destruction of the beta cells, the insulin-producing cells in the pancreas, causes the absence of insulin secretion with T1D. Researchers now believed that both genetic and environmental triggers are involved in causing the disease and does not result from diet or lifestyles[2]. Figure 1 below illustrates how the absence of insulin can affect the the uptake of glucose by individual cells.

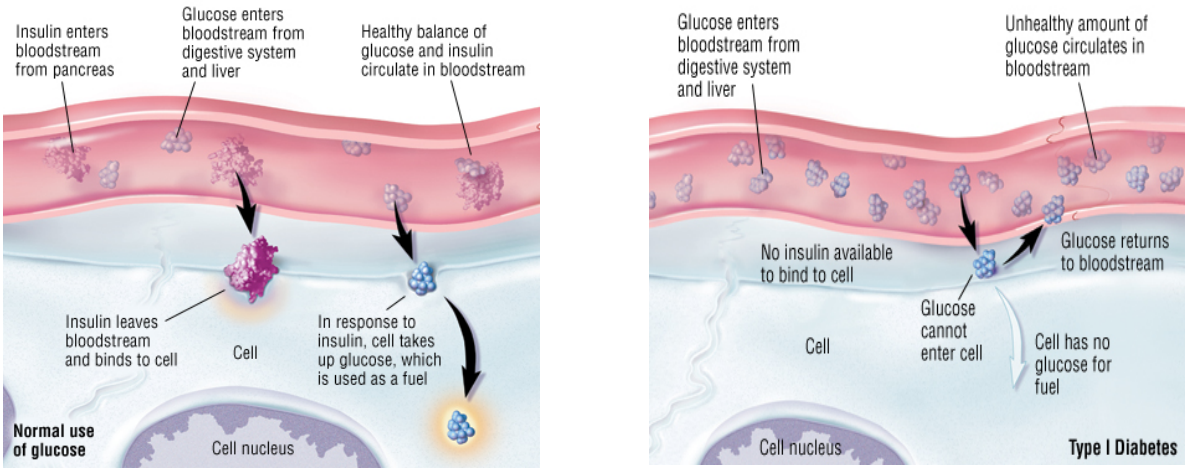

Figure 1: Diagram of normal individual to Type 1 diabetic individual. In a normal individual, the insulin allows glucose to enter the cell by binding to the cell membrane to allow transport of glucose into the cell. In a T1D individual, there is no insulin to bind to the cell membrane, and glucose cannot be transported into the cell.

As seen in the diagram, in a normal individual, the insulin binds to a receptor on the cell membrane and allow for the creation of glucose transporters that transport glucose into the cell. In an individual with T1D, there is no insulin available to bind to the receptors on the cell surface; with no insulin, glucose transports cannot bind to the cell membrane to transport glucose into the cell, so the cell cannot use the glucose for ATP generation. There is no cure for Type 1 diabetes. Current forms of treatment only seek to control the disease[3].

1.2 Current Treatment and Consequences of Treatment

The typical treatment for T1D consists of insulin intake, carbohydrate counting, frequent blood sugar monitoring, eating healthy foods, and exercising regularly to maintain a healthy weight. The goal is to keep as close to a normal blood sugar level as possible[4]. Insulin intake is performed via injections or an insulin pump[5] because oral intake of insulin results in degradation of the protein by stomach enzymes[4]. There are multiple forms of insulin, including rapid-acting insulin, long-acting insulin, and intermediate options. Insulin injections have to be taken several times a day and require

syringes and needles as well as different types of insulin depending on how much insulin is needed at a certain time of day[6]. Figure 2 below shows the different types of insulin and the conditions when they are used.

Type of Insulin & Brand Names	Onset	Peak	Duration	Role in Blood Sugar Management
Rapid-Acting				
Lispro (Humalog)	15-30 min.	30-90 min	3-5 hours	Rapid-acting insulin covers insulin needs for meals eaten at the same time as the injection. This type of insulin is often used with longer-acting insulin.
Aspart (Novolog)	10-20 min.	40-50 min.	3-5 hours	
Glulisine (Apidra)	20-30 min.	30-90 min.	1-2½ hours	
Short-Acting				
Regular (R) humulin or novolin	30 min. -1 hour	2-5 hours	5-8 hours	Short-acting insulin covers insulin needs for meals eaten within 30-60 minutes.
Velosulin (for use in the insulin pump)	30 min.-1 hour	2-3 hours	2-3 hours	
Intermediate-Acting				
NPH (N)	1-2 hours	4-12 hours	18-24 hours	Intermediate-acting insulin covers insulin needs for about half the day or overnight. This type of insulin is often combined with a rapid- or short-acting type.
Long-Acting				
Long-acting insulin covers insulin needs for about one full day. This type is often combined, when needed, with rapid- or short-acting insulin.	Insulin glargine (Lantus, Toujeo)	1-1½ hour	No peak time. Insulin is delivered at a steady level.	20-24 hours
	Insulin detemir (Levemir)	1-2 hours	6-8 hours	Up to 24 hours
Pre-Mixed*				
Humulin 70/30	30 min.	2-4 hours	14-24 hours	These products are generally taken two or three times a day before mealtime.
Novolin 70/30	30 min.	2-12 hours	Up to 24 hours	
Novolog 70/30	10-20 min.	1-4 hours	Up to 24 hours	
Humulin 50/50	30 min.	2-5 hours	18-24 hours	
Humalog mix 75/25	15 min.	30 min.-2½ hours	16-20 hours	
*Premixed insulins combine specific amounts of intermediate-acting and short-acting insulin in one bottle or insulin pen. (The numbers following the brand name indicate the percentage of each type of insulin.)				

Figure 2: Chart of the Different Forms of Insulin. There are five different forms of insulin: rapid-acting, short-acting, intermediate-acting, long-acting, and premixed. Each form of insulin has a different onset, peak, and duration. They also control blood glucose levels in different ways[6].

An insulin pump, on the other hand, is a small computerized device that delivers insulin into the body. The pump can be programmed to deliver continuous doses of insulin as well as specific doses through the day, usually around meals[7].

Both of these treatments come with their own disadvantages. While injections require less training on the part of the patient and are cheaper to purchase, low blood glucose levels can occur due to using different forms of insulin and having to self-monitor when to administer the injections. Additionally, due to frequent injections, certain parts of the body can become resistant areas where insulin will not absorb properly[8]. While the insulin pump eliminates individual injections, allows more flexibility in diet, and delivers insulin more accurately than injections, it still has some disadvantages. Since a catheter needs to be attached to the patient to deliver insulin to the body, the pump can cause diabetic ketoacidosis (DKA) if the catheter comes out and no insulin is delivered. Additionally, there is a large learning curve associated with the pump, especially for children since to learn how to properly utilize and calibrate the pump, patients need to stay overnight in a hospital or spend a whole day in an outpatient center[9]. Without proper training, patients can misuse the pump, resulting in complications that require hospitalization[10].

For glucose monitoring, there are also two options: finger-stick glucose monitoring or continuous glucose monitoring. The finger-stick method consists of taking small blood samples on test strips and using a portable meter to measure blood glucose levels. The test strip enzymes that bind glucose; the amount of enzymes bound to glucose determines the measured blood glucose level displayed on the portable meter. While this technology is improving to make blood glucose monitoring easier and faster, there are

still problems with the accuracy and specificity. For example, a true glucose level of 55 mg/dl could yield a reading as low as 40 mg/dl or as high as 70 mg/dl. The inaccuracy in the reading leads to inaccurate insulin consumption and can cause hypoglycemic or hyperglycemic states. Additionally, the glucose test strips can also be problematic depending on the enzyme present on the strip. Certain enzymes used to create the test strip do not solely bind to glucose. For example with glucose dehydrogenase pyrroloquinoline quinone (GDH-PQQ), it can bind to a number of other sugars besides glucose, causing inaccurate readings to occur with the finger-stick method. Patients do not always know what interfering sugars exist and can take glucose measurements while consuming interfering sugars. This can lead to hypoglycemia and even death if not caught early enough. There is also pain associated with having to take numerous blood samples in a day [11].

The continuous glucose monitoring (CGM) systems use a sensor inserted under the skin to check glucose levels in tissue fluid. The sensor stays in place for several days to a week, and then it must be replaced. The transmitter sends a signal from the sensor to the wireless monitor. To calibrate the device, the patient still has to use the finger-stick method. While CGM systems provide real-time measurements of glucose levels, there are more inaccurate and unreliable than the finger-stick monitors. Additionally, they are very expensive[12].

As discussed before, the goal of all T1D treatments is to maintain as close to normal blood glucose levels as possible. If a patient improperly manages their diabetes, then they can increase their risk of suffering from severe complications. T1D increases the risk for heart disease and vascular disease, heart attacks, stroke, and high blood

pressure. Excess sugar caused from improper insulin consumption can also cause neuropathy (nerve damage) since the excess sugar can damage the walls of capillaries that nourish the nerves. Kidney damage can occur since it also contains millions of tiny blood vessels that filter the blood. Severe damage can lead to kidney failure or irreversible end-stage kidney disease. Eye damage, foot damage, and skin and mouth conditions are additional complications that arise due to T1D[13].

1.3 Current Nanotechnology for Type 1 Diabetes

Knowing the problems associated with current treatments of T1D, there is a need for novel treatments to be created. A possible resource for treatment is nanotechnology; this field offers sensing apparatuses that are more sensitive, accurate, and timely. Miniature devices that deliver insulin can also be created using nanotechnology[14]. The key to developing a functional nanotechnology-based device is to create one that mimics the body's own glucose monitoring and insulin release capabilities as well as a device that does not elicit a strong immune reaction.

Currently, there are a several nanotechnology treatments being developed for the treatment of T1D. One of these new nanotechnology treatments is the microphysiometer. The microphysiometer is composed of nanotubes, which are several flat sheets of carbon atoms stacked and rolled into very small tubes. The nanotubes are electrically conductive, and the concentration of insulin in the chamber is related to the current at the electrode. These nanotubes work at physiological pH, and this sensor is able to detect insulin levels continuously by measuring the current (transfer of electrons) produced when insulin molecules oxidize in the presence of glucose. When the cells produce more insulin, the current in the sensor increases. This information can be transmitted to a wireless

computer and would allow for real time monitoring of insulin levels. This technology has the drawback of not directly measuring glucose, but rather measuring insulin.

Another technology is the implantable sensor. This uses polyethylene glycol (PEG) nanospheres covalently bound to phenylboronic acid and attached to two flurophores to monitor diabetes blood sugar levels. The nanospheres are injected under the skin and stay in the interstitial fluid; they can be seen through the skin as a tattoo. In the absence of sugar, the nanospheres are small and can maintain close contact with the fluorophores. When sugar is present, it binds to the phenylboronic acid, which increases the size of the nanospheres. The larger nanospheres are not in close contact with the fluorophores, causing the nanospheres to dim. When the nanospheres dims, the tattoo fades, indicating an increase in blood glucose levels[15].

In terms of delivering insulin, polymeric nanoparticles are used as carriers of insulin. These are biodegradable, and have polymer-insulin matrix enclosed in a nano-porous membrane. A rise in blood glucose levels causes a decrease in the size of the molecules in the nanoporous membrane, resulting in biodegradation and release of insulin. One disadvantage with this technology is that the glucose/glucose oxidase reaction causes the pH to drop in the delivery system, which causes the swelling of the polymer system, leading to more insulin than necessary being released[14]. The polymeric nanoparticles can also adhere non-specifically to surfaces they are not intended to or become trapped in the mucus linings of the body. Table 1 below summarizes the advantages and disadvantages associated with polymeric membranes and other nanoparticle membranes.

Table 1: Advantages and disadvantages of nanoparticle drug delivery systems. The systems included are polymeric nanoparticles, ceramic nanoparticles, gold nanoparticles, and liposomes.

Types of Nanoparticles	Advantages	Limitations
Polymeric nanoparticles	Degrade into biologically acceptable compounds by hydrolysis; lesser cytotoxicity, higher targeted-specificity; high level of insulin entrapment and ability to preserve insulin structure and biological activity; bypassing of the enzymatic degradation in stomach	Mucoadhesive polymeric nanoparticles may adheere non-specifically to surfaces they are not intended to (gastric mucosa, gut content) or remain trapped within the mucus
Ceramic nanoparticles	East preparative proceesses; high biocompatibilty; ultra-low size (less than 50 nm); good dimensional stability; protect the doped drug molecules against denaturation caused by changes in external pH and temperature; can be manufactures with desired size, shape, and porosity; do not undergo swelling or porosity changes	Poor permeability across the mucosal membrane and rapid mucocilitary clearance mechanism of non-mucoadhesive formulations for nsasally administered insulin
Gold nanoparticles	Long term stability in terms of aggregation and good insuln across oral and nasal mucosa; improved pharmacodynamic activity of insulin	Widespread distribution in organs like liver, lung, spleen, kidney, brain, heart, stomach, and joints
Liposomes	Biodegradable, non-toxic and non-immunogenic	Drug loading capacity remains inconclusive; captured by human body's defense system (reticuloendothelial system (RES)); post-treament

The table above also shows disadvantages for other types of nanoparticles that can be used in the delivery of insulin. While all of these nanoparticles can be used, they each have the potential to cause problems within the body, and therefore cannot yet be feasibly applied *in vivo.* Oral insulin is also a possibility if the insulin is used with polysaccharides and polymeric nanoparticles. Polysaccharides are naturally biodegradable by enzymes and have good biocompatibility. Since insulin taken orally without any membrane surrounding, it is degraded by gastric enzymes; the enveloped matrix of nanoparticles or polysaccharides are protecting it from the enzymes[14]. The oral route for insulin administration is considered to be the most convenient and comfortable, but there are still problems with using the membrane with oral insulin. Specifically, the problem is due to the intestinal epithelium being a major barrier to the adsorption of hydrophilic drugs. This

means another layer of molecules needs to be added to the membrane to allow it to function well within the intestines[14].

Considering all the disadvantages involved with current nanotechnology, there still exists a need for a novel treatment for blood glucose monitoring and insulin consumption. To address this technology gap, we look to DNA origami to create a device capable to sensing glucose and releasing insulin. The goal of this work is to take the first step in developing this device by constructing a sensor that will generally sense proteins in solution. This study will, therefore, focus on the creation and optimization of a universal protein sensor. While this protein sensor can be used to detect a glucose-enzyme complex in the treatment of T1D, the sensor can also be used to detect other proteins, such as hemoglobin.

1.4 Introduction to DNA Origami

Deoxyribose nucleic acid (DNA) consists of nitrogenous bases, five-carbon sugars, and a phosphate group. The structure DNA is shown in Figure 3 below.

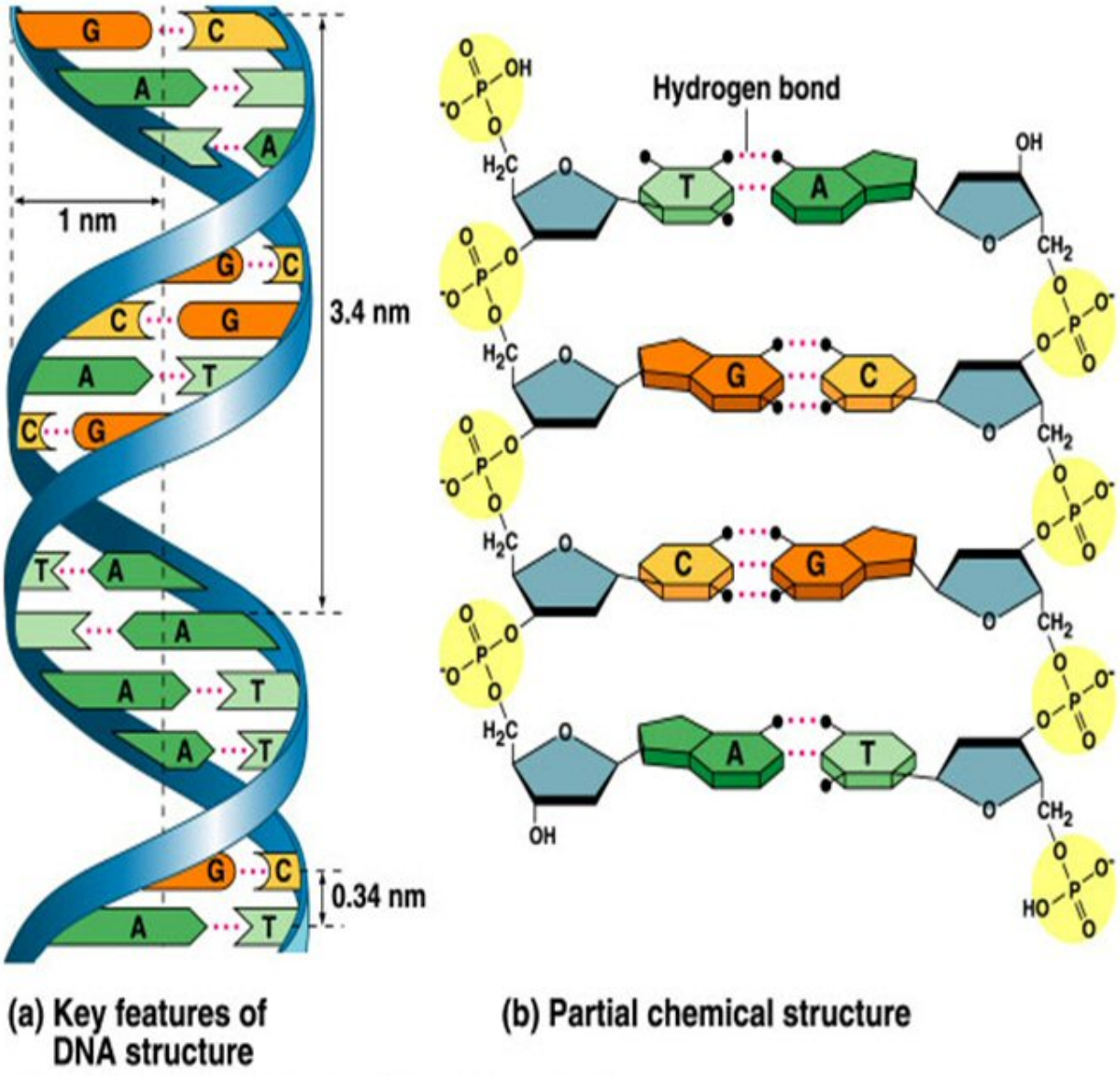

Figure 3: The structure of DNA. The structure is well-defined with specific base pairing and helix turns. As shown, adenosine binds with thymine, and guanine binds with cytosine. Each helix turn is about 3.4 nm[16].

Foremost, DNA is known for encoding genetic information, but it also contains properties that allow it to be a good foundation for nanotechnology. Recently, DNA origami has emerged as a promising technique for assembling complex nanostructures. The design of DNA-based nanostructure relies heavily on the assembly properties of the bases. The field of DNA nanotechnology was originally established by Nadrian Seeman's, a chemist and crystallographer at NYU. He explored junctions and lattices of

nucleic acids and initially demonstrated DNA nanoconstruction through the fabrication of a DNA molecular cube[17,18].

Scaffold DNA origami, developed by Paul Rothemund in 2006, has dramatically widened the scope of DNA nanotechnology. In this approach, many short single-stranded DNA ("staples") direct the folding of a long, circular single-stranded DNA ("scaffold") into different structures. It is the sequences of the staples that will determine the final shape of the nanostructure. The scaffold is typically derived from the single stranded genome of the M13MP18 bacteriophage. A solution containing the scaffold and staples are heated to facilitate annealing in a thermal ramp. This method allows for high yield assembly of nanostructures with significantly greater geometric complexity than previous approaches. The first structures created with DNA origami included squares, rectangles disks, and five-pointed stars with dimensions in the 10-100nm range with a spatial resolution of 6 nm. As the technology continued to expand, modular "DNA jigsaw pieces", nano-sized breadboards as templates for nanomaterials, and even three-dimensional nanostructures have been made by stacking layers of double helices in a honeycomb or square lattice. Figure 4 below shows some of the structures originally created by Paul Rothemund using this technique[19].

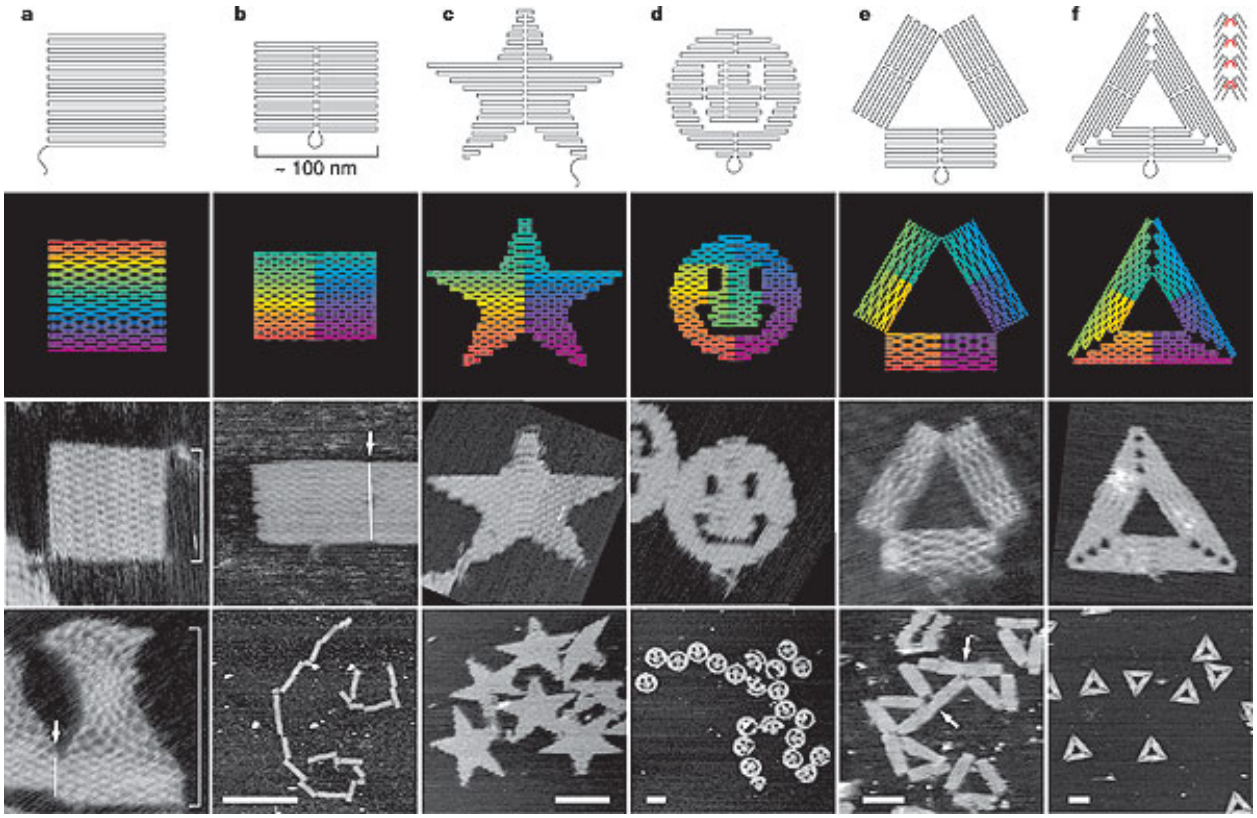

Figure 4: DNA Origami structures created by Paul Rothemund. The shapes include stars, smiley faces, triangles, and two differently routed rectangles. This shows the versatility of DNA Origami in producing unique nanostructures

As shown in the figure, there are many options for creating structure using DNA origami. Recently, DNA nanotechnology has even demonstrated immense promise for applications such as drug delivery. The Trojan Horse developed by the Nanoengineering and Biodesign Lab (NBL) has proven to be an effective approach to circumvent drug resistance in leukemia cells. The structure is able to enter cells via endocytosis and bypass defenses in the cell membrane against the free drug[20]. Additionally in 2012, Shawn Douglas developed an autonomous DNA nanorobot that could deliver a payload to cells upon triggered activation[21]. As the field grows, a major focus is developing tools to track and treat diseases such as diabetes.

1.5 Significance

As of 2011, 266 million people worldwide are affected by Type 1 diabetes, and this

number is expected to rise to 552 million by 2030. In the United States, diabetes is the 7th leading cause of death. Additionally, it can increase the risk of heart disease by 2-4 times, lower life expectancy by up to 15 years, and is the leading cause of kidney failure, lower limb amputation, and adult on set blindness. The estimated financial cost of diabetes is the US in 2007 was $174 billion, which includes the costs of premature death, disability, and medical care. In 2012, the cost increased to $249 billion[22]. Additionally, more and more people are being diagnosed with diabetes. The incidence of the disease in young people to set to increase by 49% over the next 40 years[23]. Diabetes research can significantly improve the quality of life and the life expectancy of people diagnosed with Type I diabetes. In last 50 years of diabetes research, researchers have found ways to produce human insulin from microorganisms, develop insulin pumps to deliver continuous insulin to patients to help avoid hypoglycemia, and invent a non-invasive A1C, which measures average blood glucose levels over a three-month period. Further research into the establishment of a continuous glucose monitor and insulin delivery sensor can significantly improve the economic costs and the human costs of this disease; more people suffering from diabetes would be able to live longer and reduce complications that arise from diabetes[24]. More broadly, the creation of a protein biosensor would mitigate the high demand for methodologies for detecting and identifying specific proteins in biological and environmental samples.

1.6 Thesis Objective and Hypothesis

The objective of this thesis is to develop and optimize a universal protein sensor than can eventually be applied to a glucose-protein complex in the measurement of blood glucose levels needed for T1D. The creation of a protein sensor with DNA origami offers

many advantages over other nanotechnologies. DNA origami offers unprecedented control over nanoscale geometry and biochemical function as well as controlled delivery of medicine and fluorescent-based imaging applications[25]. By creating a protein sensor through DNA origami, there is inherent biocompatibility and absence of cytotoxicity. The protein sensor will also alleviate some of the struggles and complications associated with T1D since the protein sensor will be able to mimic natural glucose monitoring mechanisms in the body.

The study looks at two configurations of the DNA protein sensor as well as two different environmental conditions. The protein sensor is tested with thrombin, a protein used in blood coagulation, because of how highly studied the protein is and its availability. It is hypothesized that the protein sensor will work well in both closed-to-open configuration and the open-to-close configuration, and the protein sensor will work better in the buffer most consistent with physiological conditions. Ultimately, the optimization of this device will allow for further application with glucose.

1.7 Thesis Overview

This thesis includes four chapters. Chapter 1 is the relevant background and motivation for the project. Chapter 2 covers methodology, and chapter 3 details the results. Chapter 4 includes conclusions and future work. References are included at the end of the document, and there is a table of figures and tables in the front of the document.

Chapter 2: Thrombing-Binding Protein Sensor Methodology

2.1 Modification of structure

The original DNA structure, the hinge, was designed in the Nanoengineering and Biodesign Lab (NBL). The hinge consists of two stiff bundles of 18 double-stranded DNA helices connected at one end by 6 single-stranded connections. The hinge is known to show resistance to small and large angles and has relative flexibility in the range between 40° and 80°[26]. The structure was designed used caDNAno and is shown below in Figure 5.

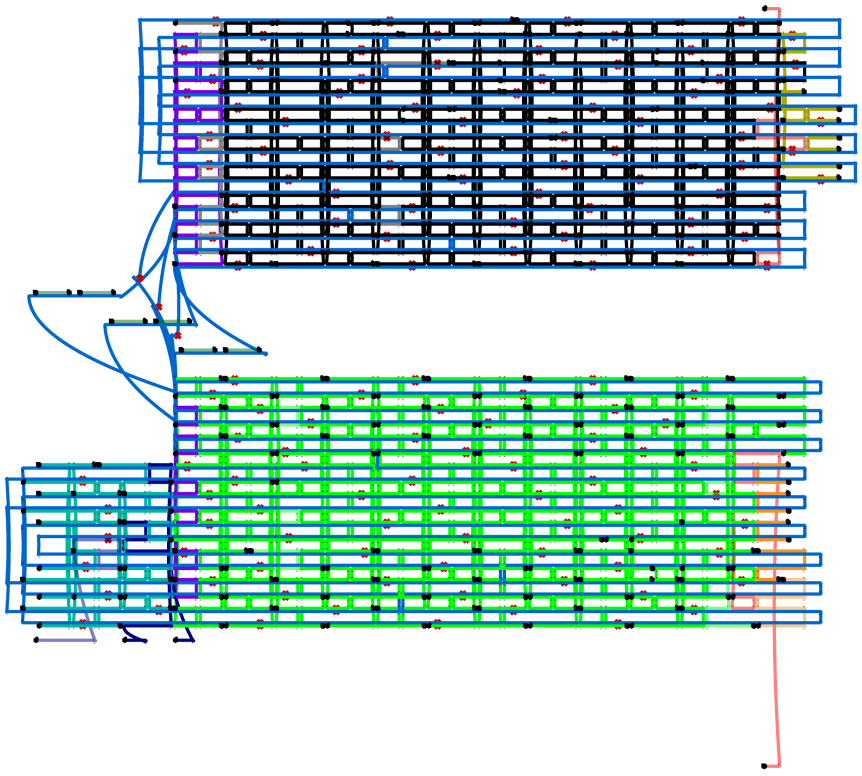

Figure 5: caDNAno 2 Design. The hinge is composed of different staples and is shown in different colors. The structure was originally designed by Alexander E. Marras in the Nanoengineering and Biodesign Lab

The structure was then modified to act as a universal protein sensor through the use of overhanging staples and aptamers (short ssDNA sequences that bind to pre-selected

targets, such as proteins with high specificity and affinity[27]). The modification depends on the configuration of the hinge. There are two configurations used: the closed default hinge and the open default hinge. The closed default hinge is shown in Figure 6 below.

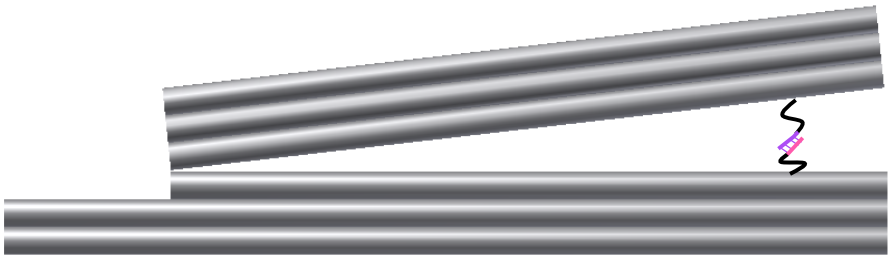

Figure 6: The Closed Default Hinge. The hinge contains one thrombin-binding aptamer (purple) and a complimentary sequence to the aptamer (pink). The binding of these two DNA sequences causes the hinge to be closed in the absence of thrombin.

The figure shows two complimentary strands that are bound to each in their natural state. The purple strand is the thrombin-binding aptamer while the pink strand is a complementary sequence. In the absence of thrombin these two sequences bind to each other and cause the hinge to remain closed. The aptamer and its complementary sequence are located at the end of two overhanging staples that come off the arms of the hinge.

The opened default hinge is shown in Figure 7 below.

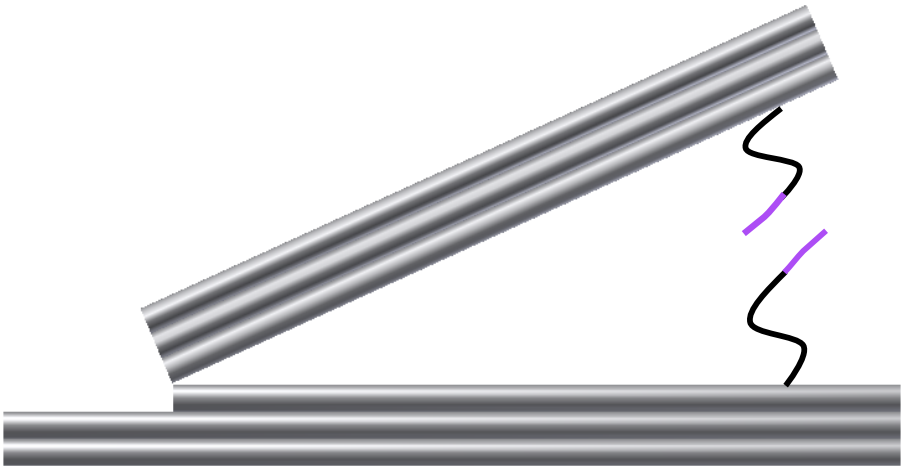

Figure 7: The Opened Default Hinge. The hinge contains two thrombin-binding aptamers (purple). The aptamers are not complementary to each other, causing the hinge to remain open.

The figure shows two thrombin-binding aptamers (purple) located on the overhanging staples of the arms of the hinge. The aptamers are not complementary to each other, and therefore, all the hinge to stay in the open position in the absence of thrombin.

2.2 Thrombin-binding Aptamer

The thrombin-binding apatamer (TBA) is shown in Figure 8 below.

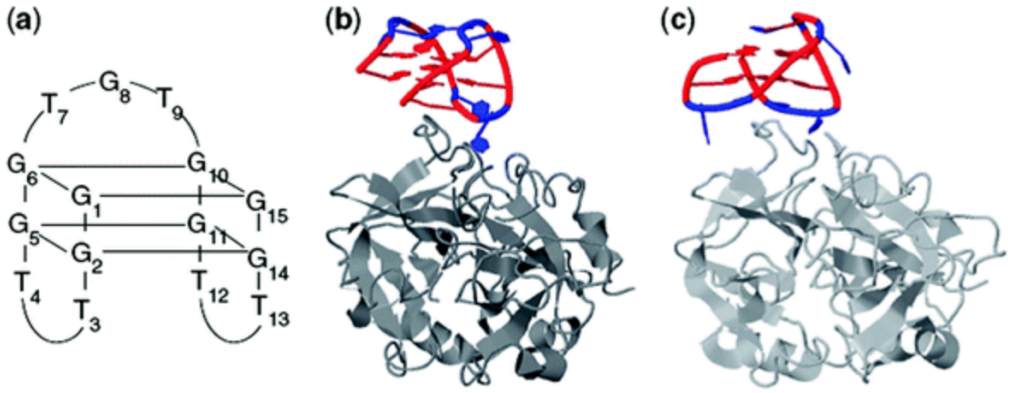

Figure 8: Diagram of the Secondary Structure of the TBA and Its Interaction with Thrombin. (A) shows the secondary structure of TBA. (B) and (C) show the interaction of TBA with the thrombin anion exosite I according to X-ray and NMR, respectively[28].

In Figure 8, (A) show the secondary structure of the TBA. This structure, as shown in (B) and (C), can attach to multiple amino acids via hydrogen bonding in a binding pocket of thrombin. This binding of TBA to thrombin allows the aptamer to be used as signaling system to indicate the presence of thrombin in solution. Any modifications to the secondary structure of TBA or the binding pocket of thrombin leads to poor or no binding.

2.3 Folding Reaction, Characterization, and Purification

The hinge was folded using previously defined methods[29]. The scaffold used was an 8064 base scaffold; it is a variant of the M13MP18 circular ssDNA genome. The scaffold is placed in solution at final concentration of 20 nM in a folding buffer containing 0.5x Tris and EDTA (TE), 5 mM NaCl, 18 mM $MgCl_2$, and water as well as the designed staple strands that are ordered commercially. Each staple is placed in the solution at a 10-fold excess at 200 nM compared to the scaffold. An 18 hour and a 2.5 day thermal ramp were run on separate folding reactions. Each thermal ramp involves rapid heating to 65°C and slowly cooling to 4^{O}C to facilitate the self-assembly process. The folding reaction was subjected to agarose gel electrophoresis to determine if the products were well-folded nanostructures. Based on the degree of folding, an optimal thermal ramp could be chosen.

Following this characterization via gel electrophoresis, multiple solutions with scaffold and staples were folded again using the optimal thermal ramp. The products of the folding reaction were then purified to remove the excess staple strands. This involved adding an equal volume of 15% polyethylene glycol (PEG) 8000 into the folding reaction and centrifuging at 1600g for 30 minutes at 4°C. The PEG polymers act as a separating

agent and cause the excess staples to separate from the DNA Origami structure in the solution[30]. The supernatant containing the excess staples was removed, leaving behind a pellet containing the folded structure. The pellet was resuspended in a solution of 10 mM TE and 18mM $MgCl_2$.

2.4 Gel Electrophoresis

Agarose gel electrophoresis was used to initially verify properly folded structure. The folding reaction was run through a 2% agarose gel in the presence of 0.5X TBE and 11mM $MgCl_2$. The gels were run at 70V for 4 hours to allow time for band separation. The resulting gel was imaged and certain bands were excised for Transmission Election Microscopy (TEM).

2.5 Transmission Electron Microscopy

To further understand the degree of folding and functionalization, the nanostructures were imaged via transmission electron microscopy (TEM). The products of the gel electrophoresis were placed on copper mesh grids and negatively stained with Uranyl Formate (UFo)[29]. 3.40 μL of the sample was placed on the grid and incubated for 4 minutes. The sample was wicked away and negatively stained with 10 μL and 20 μL of UFo. The UFo was incubated for 10 seconds before being wicked away. A FEI Tecnai G2 Spirit TEM, which uses and electron acceleration voltage of 80kV, was used to image the nanostructures. The structures were images at 50,000x magnification.

2.6 Buffer Conditions

To understand ideal buffer conditions for the thrombin protein sensor, two different buffers were made. The resuspension buffer was the foundation of the two buffers, and it contained 2M Tris-HCl, 1.375 mM $MgCl_2$, Bovine Serum Albumin (BSA)

and enough Phosphate-Buffered Saline (PBS) for a total volume of 50 mL. For the binding buffer containing 140 mM NaCl, 2.762 mL of the resuspending buffer was added to .0492 mL of 4 M NaCl. For the binding buffer containing 200 mM NaCl, 2.671 mL of the resuspending buffer was added to .140 mL of 4 M NaCl. The 140 mM NaCl concetration was chosen because proteins are at their optimal functionality at this concentration and below. The 200 mM NaCl concentration was chosen because DNA irigami structures are at their optimal functionality at this concentration to up to 2 M NaCl. 2.811 mL of pure thrombin were added to each binding buffer to obtain a concentration of 10mM thrombin in solution. The thrombin-binding buffers were then aliquoted into specific volumes, flash frozen, and placed in a -80°C freezer for future use. Folding reactions were run again through an ideal thermal ramp, and the PEG products were resuspended this time in each of the binding buffers. Thrombin titrations were then done to see the effects of thrombin on each of the sensors.

2.7 Thrombin Titrations

To titrate the thrombin with the DNA protein sensors, a serial dilution of thrombin was first completed. An allotment of thrombin-binding buffer was taken from the freezer and diluted in either the 200 mM NaCl binding buffer or the 140 mM NaCl binding buffer. The dilutions were as follows: 10mM thrombin, 1 mM thrombin, 100 μM thrombin, 10 μM thrombin, 6 μM thrombin, 600 nM thrombin, 200 nM thrombin, 60 nM thrombin, 20 nM thrombin, and 2 nM thrombin. The titrations placed equal volumes of the protein sensor and the thrombin in solution to obtain the following solutions: 300 nM thrombin, 100 nM thrombin, 30 nM thrombin, 10 nM thrombin, and 1 nM thrombin. The degree of functionalization of the sensor was then recorded through TEM imaging.

2.8 Angular Distributions

In the presence of thrombin, the Closed Default Hinge should open as shown in Figure 9 below.

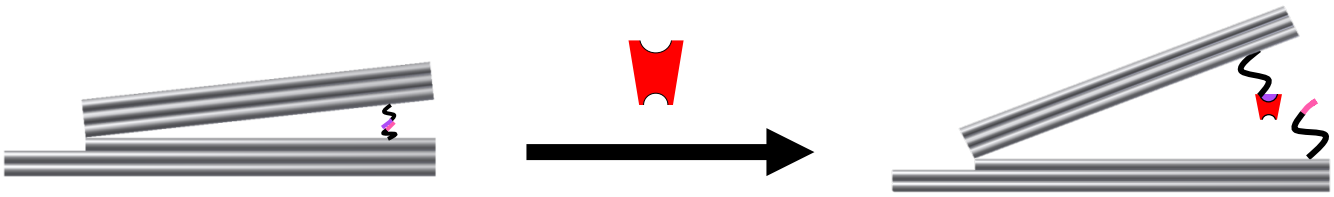

Figure 9: The Closed Default Hinge in the Presence of Thrombin. The Closed Default Hinge is introduced to thrombin (red) in solution. The thrombin then binds to the thrombin aptamer and opens the Closed Default Hinge.

In the figure above, the thrombin (red) is introduced to the hinge in solution. The half circle shown in the figure indicates the necessary secondary structure formation of the aptamer to bind to thrombin. The thrombin binds to the thrombin-binding aptamer (purple), which causes the thrombin-binding aptamer to unbind from the complementary sequence (pink) on the other overhanging staple. This allows the hinge to open.

In the presence of thrombin, the Opened Default Hinge should close as shown in Figure 10 below.

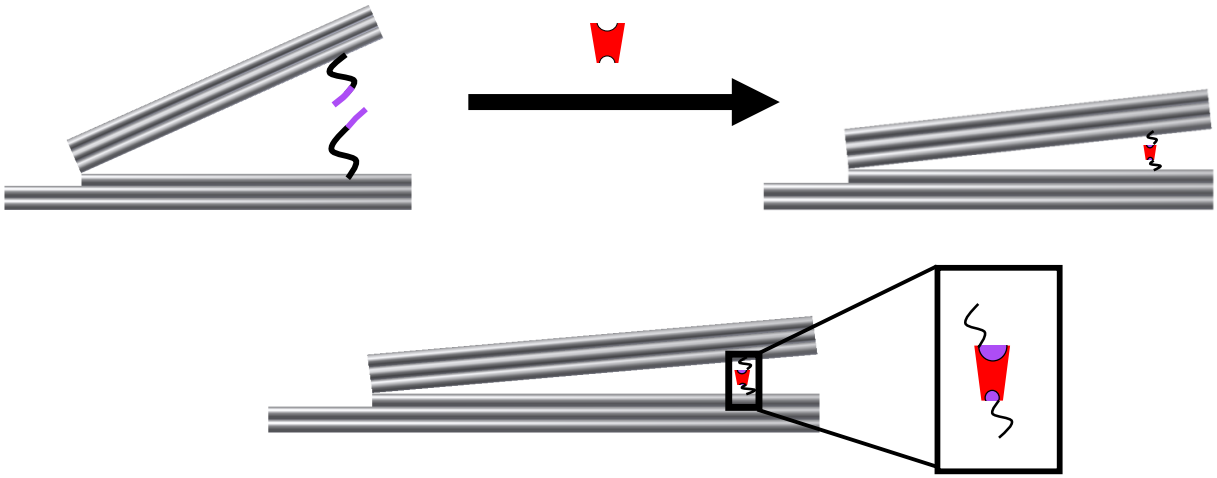

Figure 10: The Opened Default Hinge in the Presence of Thrombin. The Opened Default Hinge is introduced to thrombin (red) in solution. The thrombin then binds to the two thrombin aptamers (purple) and closes the hinge.

In the figure above, the thrombin (red) is introduced to the hinge in solution. The thrombin binds to the thrombin-binding aptamers (purple), which causes the two arms of the hinge to come together. This causes the hinge to close.

To ensure there was a baseline comparison when changes were made in thrombin concentration, a control hinge was also designed. This control hinge is shown in Figure 11.

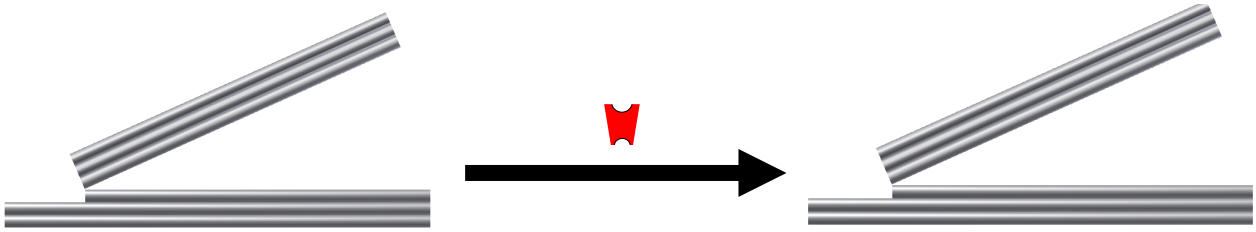

Figure 11: The Control Hinge in the Presence of Thrombin. The Control Hinge is introduced to thrombin (red) in solution. The thrombin has no place to bind, and therefore, there is not configurational change in the Control Hinge

In the figure above, the thrombin (red) is introduced to the hinge is solution. This hinge contains no thrombin aptamers or overhanging staples. This means that even in the presence of thrombin, there will be no change in the configuration.

To test the functionality and optimize the protein sensor, the hinges were introduced to the thrombin titration solutions. Images of the hinges were taken on the TEM after they interacted with thrombin, and individual angles of the hinges were measured using the angle measuring tool in ImageJ. The individual measurements were complied to create distributions in MatLab. The distributions from each configuration were compared against each other to understand the changes resulting from buffer conditions and the presence of thrombin.

Chapter 3: Results and Discussion

3.1 Gel Electrophoresis

Gel electrophoresis separates structures based on size. The smaller structures will run through the gel faster than the larger structures. Looking at the differences in separation, we can tell if the hinges are well folded.

Figure 10 below shows the results of the 18-hour thermal ramp used to fold the DNA origami.

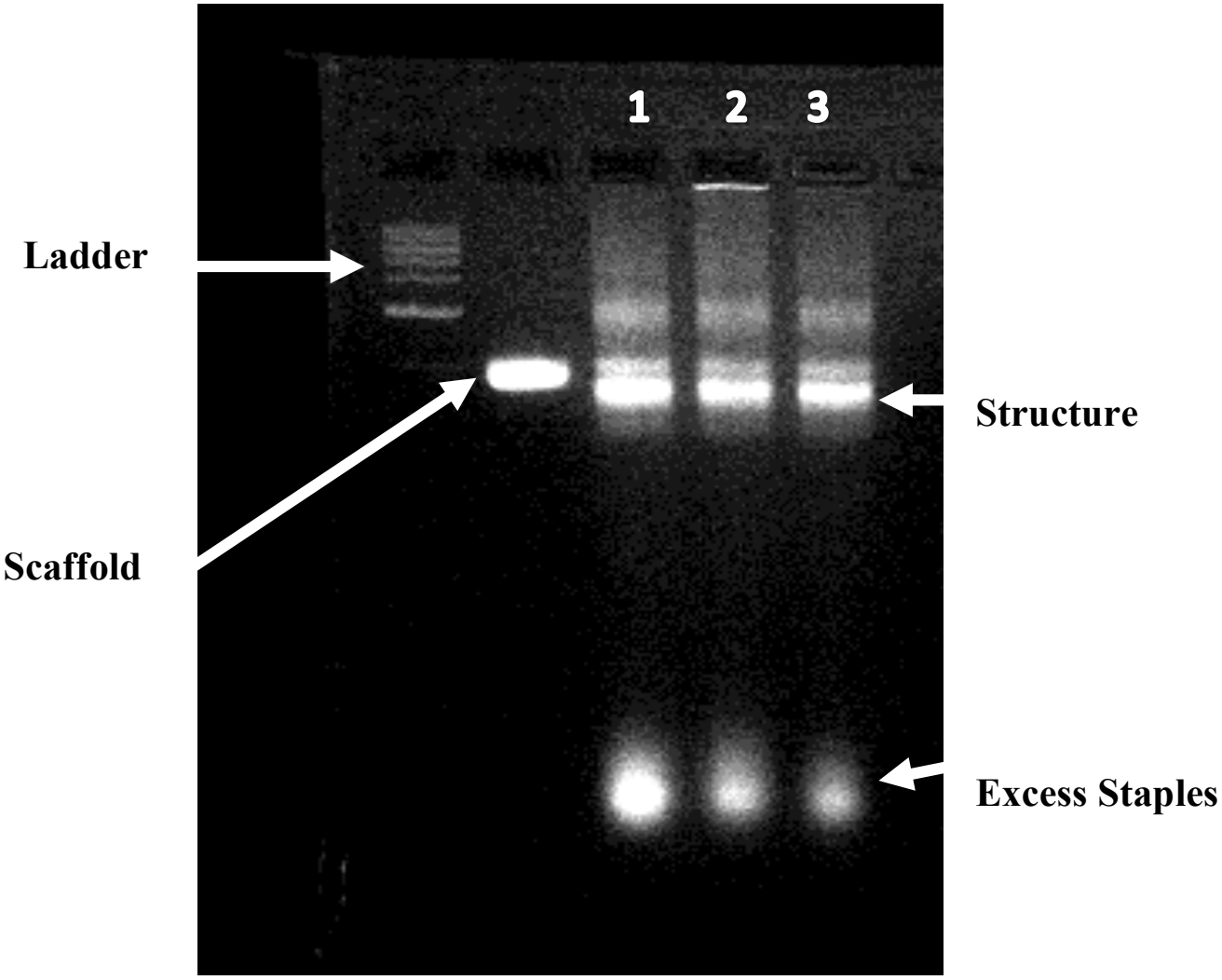

Figure 12: Gel Electrophoresis for Structures Folded in 18-hour Thermal Ramp. The three different hinges are folded in an 18-hour thermal ramp. A sample of the folded structures are placed in individual wells to test how well folded the structures are. 1 refers to the control hinge, 2 refers to the closed default hinge, and 3 refers to the opened default hinge.

The gel pictured in the figure above shows the accuracy of folding for each of the three different configurations of the hinge. The Control Hinge is in the lane marked 1, the Closed Default Hinge is in the lane marked 2, and the Opened Default Hinge is in the lane marked 3. On the far left of the gel, a 1kb ladder was run as a reference. A scaffold of 8064 bases was run on the next lane to also act as a reference point for the folded structures. The farthest and brightest band at the end of the gel corresponds to the excess staples, which are much smaller than the other structures. This gel shows there are three bands coming from lanes 1-3. The first and the second band from the top show improper folding; the third, fastest-running, and brightest band shows well-folded structures. This band moves slightly farther than the scaffold because the folded structures are more compact than the scaffold. This gel indicates that the hinges are folded well and that they can be folded using an 18-hour thermal ramp.

Figure 13 below shows the results of a 2.5-day thermal ramp.

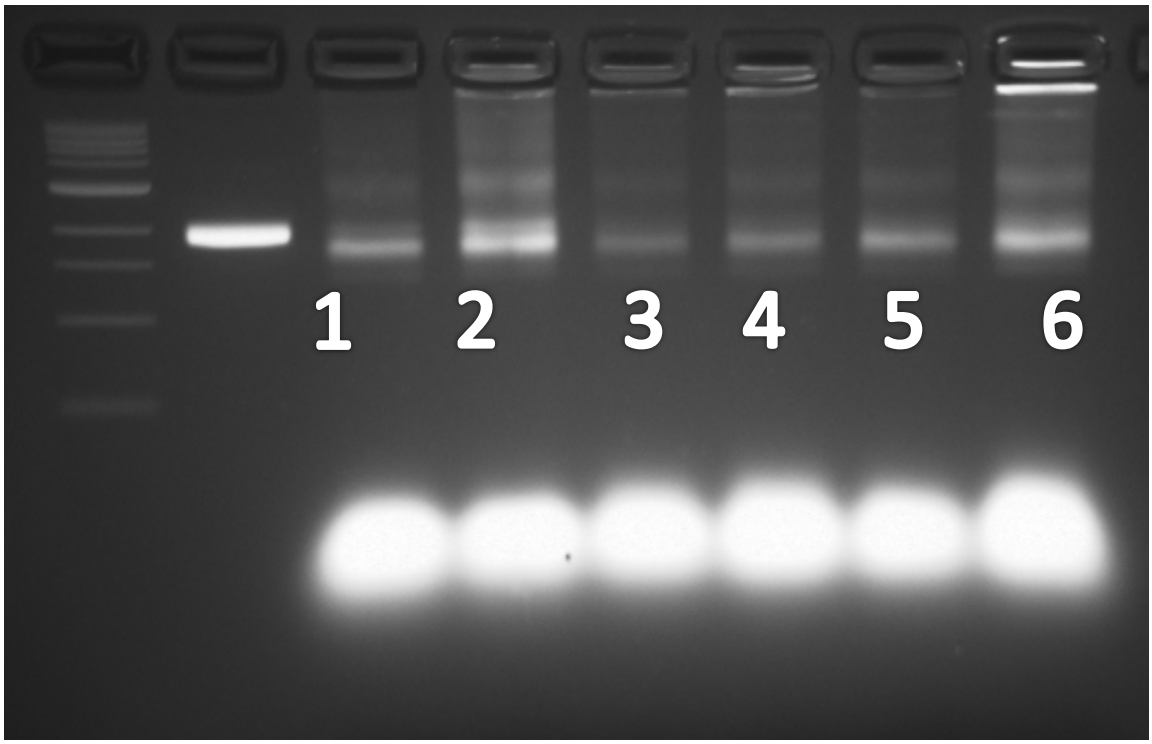

Figure 13: Gel Electrophoresis for Structures Folded in 2.5 Day Thermal Ramp. The gel is run to test how well folded the strucutres are. Lanes 1 and 2 refer to the Control Hinge. Lanes 3 and 4 refer to the Closed Hinge, and lanes 5 and 6 refer to the Opened Hinge

The gel pictured in the figure above contains a 1 kb ladder and 8064 scaffold run in the second lane. Lanes 1 and 2 contain the Control Hinge, lane 3 and 4 contain the Closed Default Hinge, and lane 5 and 6 contain the Open Default Hinge. There again exists a bright narrow band corresponding to each well that contains the structure that shows well folded structures. There is another band above the bright and narrow band that shows improper folding. Overall, this gel indicates the structures are well folded, but not significantly better folded than they are using an 18-hour thermal ramp.

3.2 Transmission Electron Microscopy Results

To verify the well folded structure, the gel bands were excised and imaged under TEM. Figure 14 below shows the results of imaging one of the gel bands.

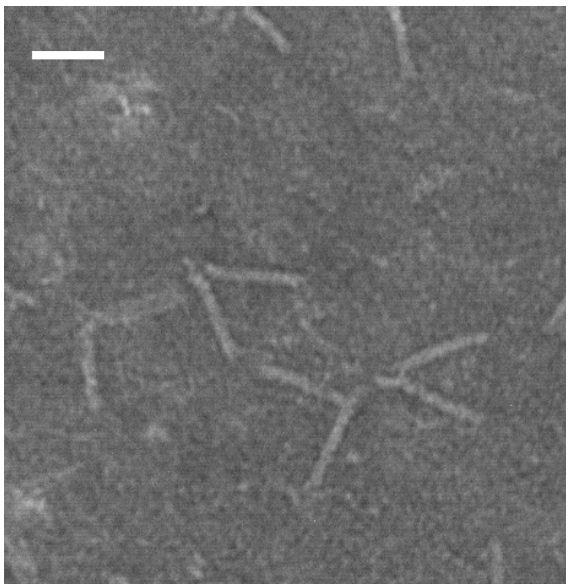

Figure 14: TEM Image of Gel Band from Open Default Hinge in 18-hour Ramp. The hinges here are open in the absence of thrombin and show that the structures are well folded and functional. Scale bars 50 nm.

In the figure above, the TEM allows for visualization of the structures to determine if they are well folded. The image shows the Opened Default Hinge after an 18-hour thermal ramp. The hinge is in the open position as well as in the proper form of the hinge. This image reconfirms the use of an 18-hour thermal ramp to fold the structures.

The TEM is also used to image the results of the thrombin titration solutions. Figure 15 below shows the result of placing the Control Hinge in the thrombin titration solutions containing 140 mM NaCl.

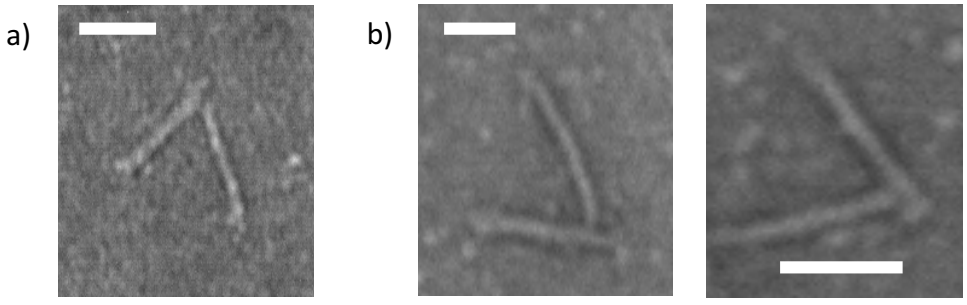

Figure 15: The Control Hinge in 140 mM Nacl Solution with 0 nM thrombin and 10 nM thrombin. A depicts the Control Hinge with there is no thrombin is in solution and B represents when there is 10 nM thrombin in solution. Scale Bars 50nm

The figure above shows the Control Hinge when no thrombin is present (left) and when 10 nM of thrombin (middle and right) is present in solution. Under the TEM, the hinge does not change configuration when thrombin is added, which verifies the functionality of the Control Hinge.

Figures 16 and 17 below show the Closed Default Hinge and the Opened Default Hinge in the 140 mM solution when thrombin is present and when thrombin is absent.

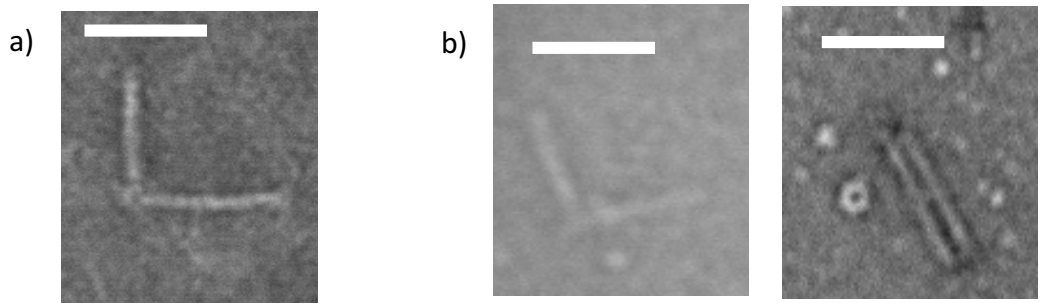

Figure 16: The Opened Default Hinge in 140 mM NaCl solution with 0 and 30 nM thrombin. (A) depicts when there is no thrombin and (B) depicts when there is 10 nM of thrombin in solution. Scale Bars 50nm

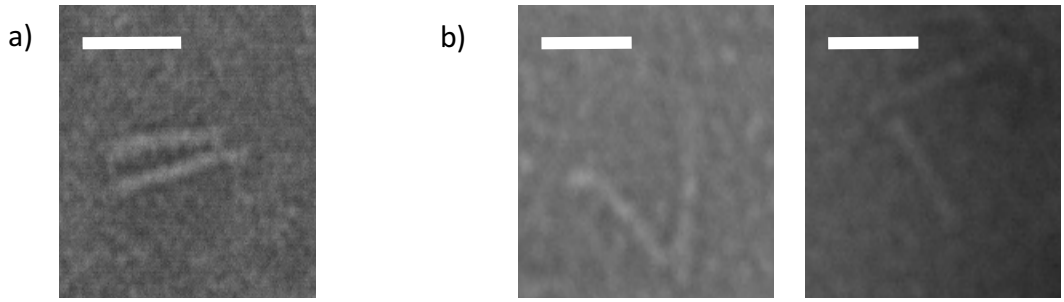

Figure 17: The Closed Default Hinge in 140 mM NaCl solution with 0 and 30 nM thrombin. (A) depicts when there is no thrombin and (B) depicts when there is 10 nM of thrombin in solution. Scale Bars 50nm

Figures 16 and 17 show the Opened Default Hinge and Closed Default Hinge when there is no thrombin present (left) and when 30 nM of thrombin is present (middle and right). The TEM image shows that most Opened Default Hinge structures are open when there is

no thrombin present. Not all the structures were open, however, and this could be due to the presence of misfolded structures. TEM images of the Closed Default Hinge show mostly closed when no thrombin is present. The presence of open structures could be due to the location of the aptamers on the hinge. Also the open hinge has a wide range of motion (from 0° to 180°); the hinge will not close if the aptamer is not in close proximity to the complementary sequence, leading to open structures. The Opened Default Hinges does show evidence of closing when thrombin is introduced, but there are still open structures. The Closed Default Hinge opens when the thrombin is introduced, and while there are closed structures present, there did not appear to be as many nonfunctional structures are there were with the Open Default Hinge. The presence of nonfunctional structures in thrombin solutions prompted the need to further characterize the degree of functionality of the Closed Default Hinge and the Opened Default Hinge.

3.3 Angular Distribution Results

To quantitatively characterize the different configurations of the hinges, angular distribution measurements were made using ImageJ. This is show in Figure 18.

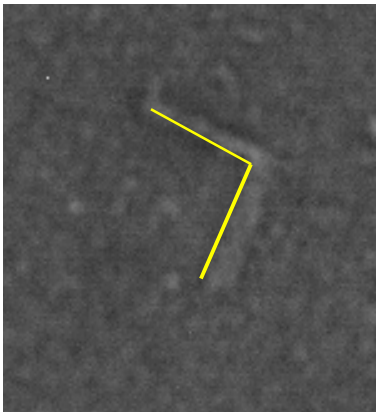

Figure 18: TEM Image with Angle Measurement.

The individual angle measurements of the TEM images where complied in Matlab. These angle measurements were then used to plot an angular distribution of each hinge configuration in the presence and absence of thrombin. Figures 19, 20, and 21 show these angular distributions of the different configurations of the hinge in 140 mM NaCl.

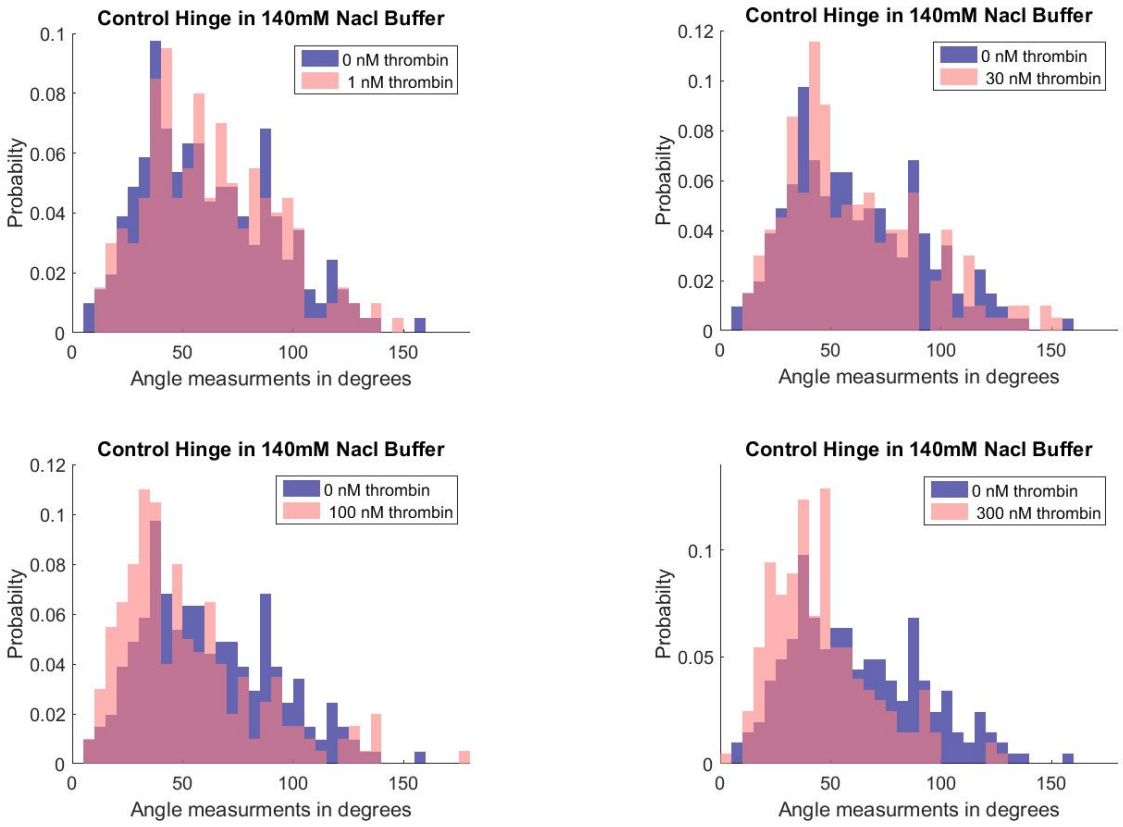

Figure 19: The Angular Distribution of the Control Hinge in 140 mM NaCl in Different Thrombin Concentrations. The distributions of the figures do not change as the thrombin concentration is increased.

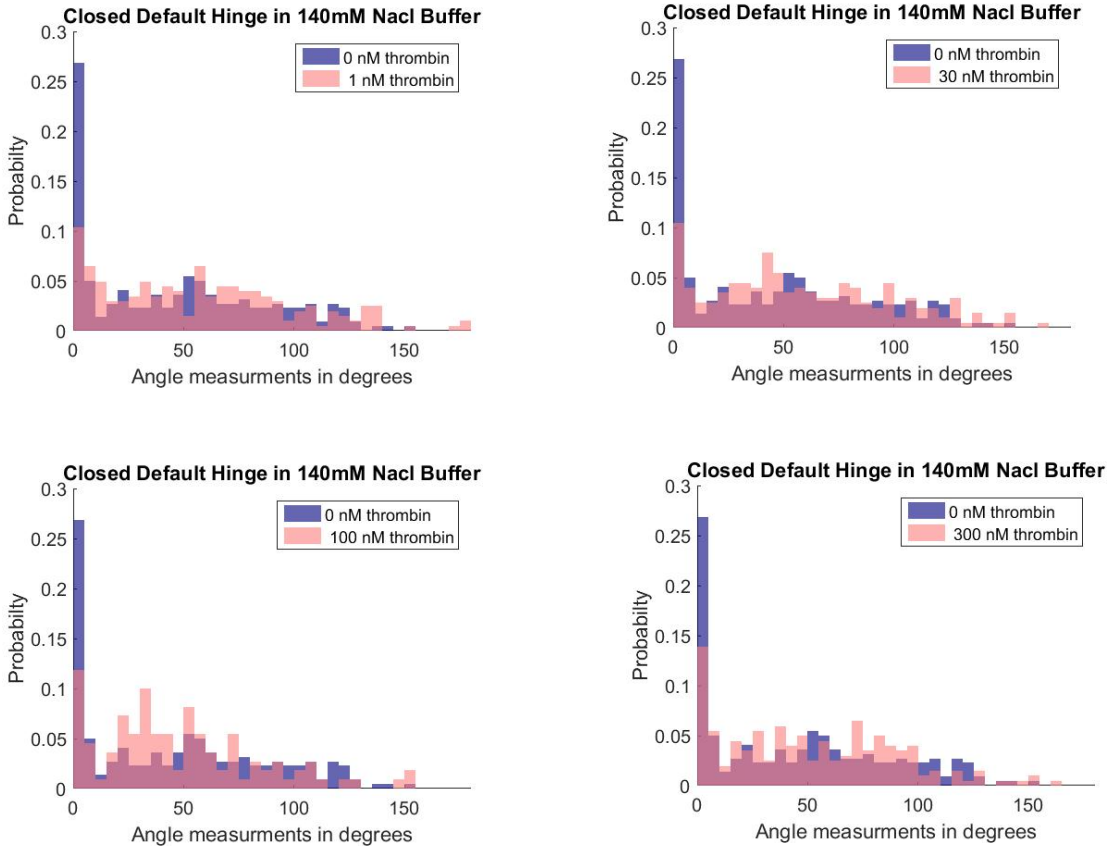

Figure 20: The Closed Default Hinge in 140 mM NaCl in Different Concentrations of Thrombin. The distribution shows a shift to the right as the thrombin concentration increases.

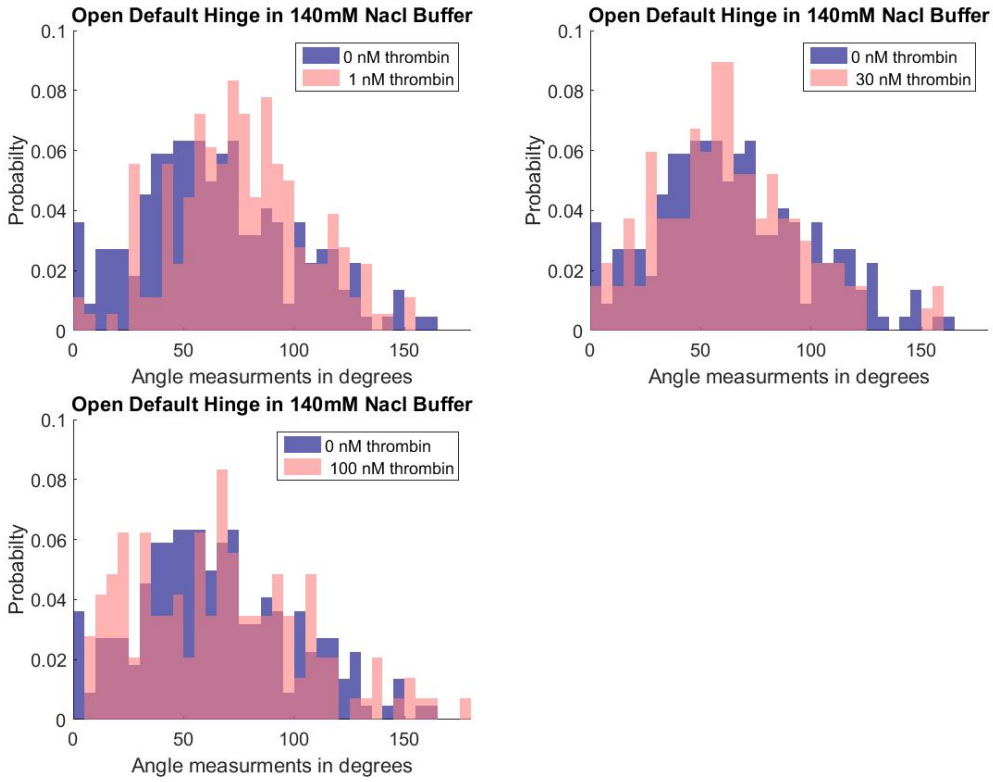

Figure 21: The Opened Default Hinge in 140 mM NaCl in Different Concentrations of Thrombin. The distributions either stay the same or shift to the right as the thrombin concentrations increase.

Figure 19 shows the distribution of the Control Hinge doesn't change as the concentration of thrombin is increased. This shows that this hinge functions correctly and that the DNA origami structure itself is not affected by the presence of the protein. Figure 20 shows the distribution of the Closed Hinge shifts to the right as the concentration of thrombin increases. The Closed Default Hinge should not have a wide distribution (ranging from 10° to 180°) when no thrombin is present because all Closed Default Hinge structures should have an angular measurement of under 10°. Normally, an open hinge has a large angular distribution/motion. This shows we do not have a high efficiency of closing. The presence of this wide distribution results from the hinge's inability to move into a position where it was possible for it to close. The connections on the vertex of hinge can be too stiff for the hinge to have a large range of motion, causing

the hinge to average around 50°. However, when thrombin is present, the "under 10°" angular distribution decreases and the probably of the "10° to 180°" angular distribution increases. This is what is noted as a shift in distribution, and this shows that this hinge functions correctly and is able to sense when thrombin is in solution. The hinge also shows slight sensitivity to the concentration of thrombin in solution. Figure 21 shows the distribution of the Opened Default Hinge doesn't change or shifts to the right as the concentration of thrombin increase. This shows that this hinge does not function correctly because the hinge does not close as it should when thrombin is introduced. The distributions for the Control and Closed Default Hinge also show that the buffer conditions work well, indicated by the presence of uniform distribution of the Control Hinge and a shift in distribution of the Closed Default Hinge, for the hinge functionality.

Figures 22, 23 and 23 show the angular distributions of the hinge at different concentrations of thrombin in 200 mM NaCl.

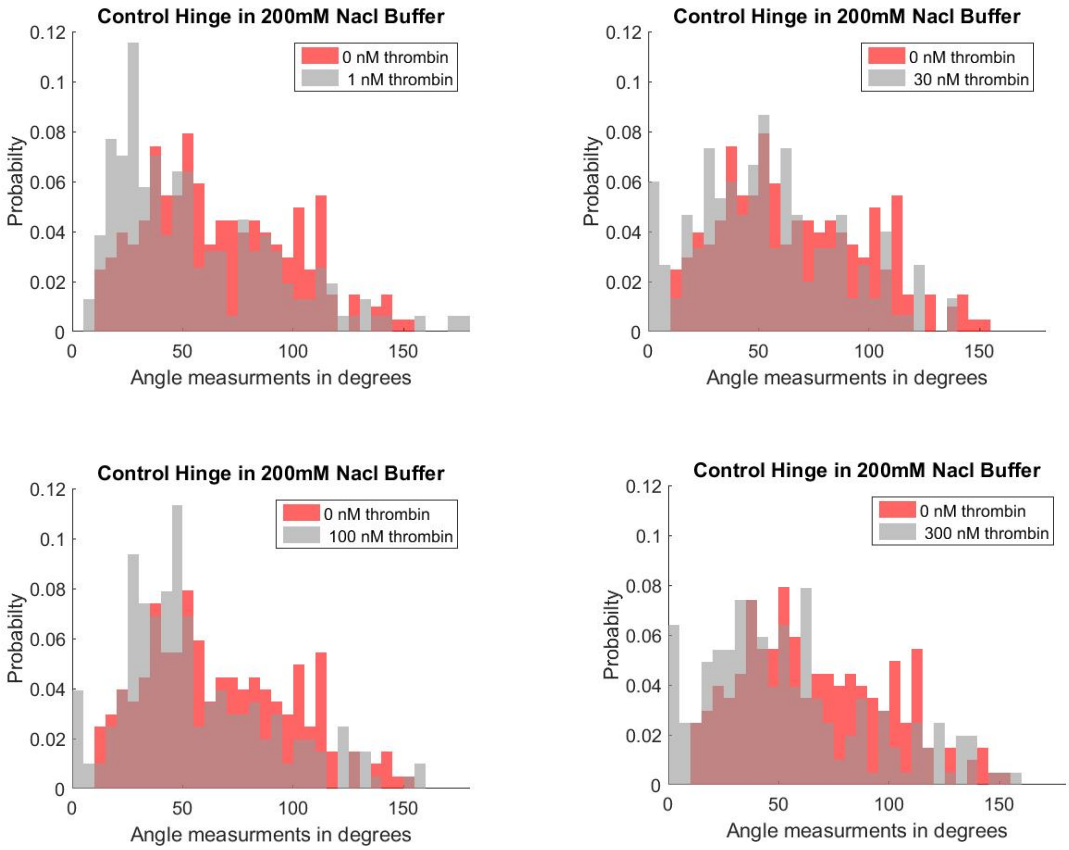

Figure 22: The Angular Distribution of the Control Hinge in 200 mM NaCl in Different Thrombin Concentrations. The distributions of the figures do not change as the thrombin concentration is increased.

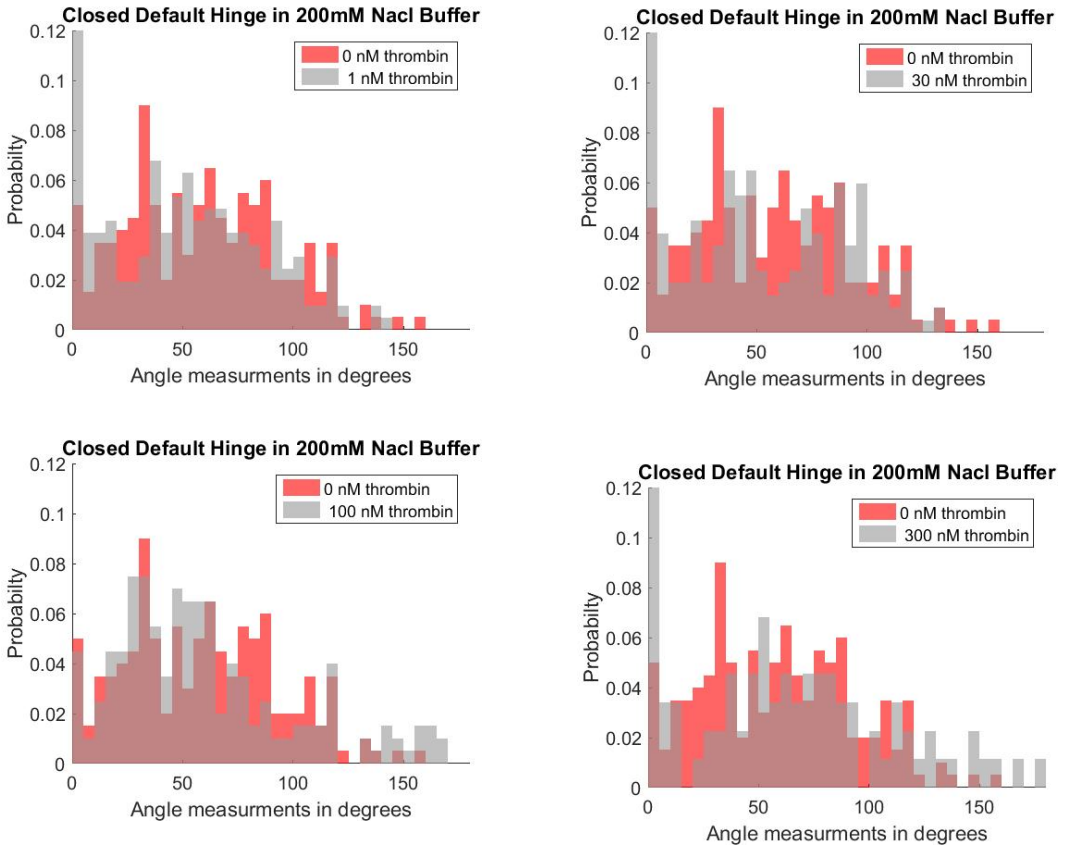

Figure 23: The Closed Default Hinge in 200 mM NaCl in Different Concentrations of Thrombin. The distribution shows a shift to the left as the thrombin concentration increases

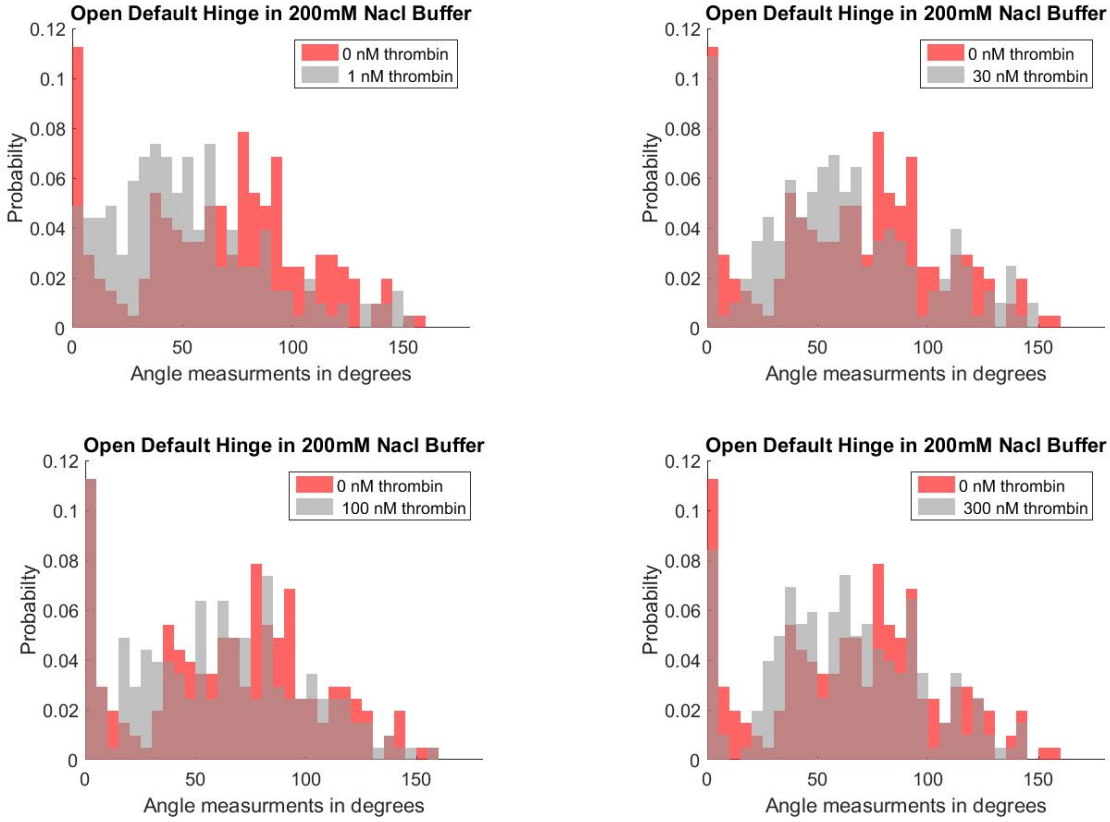

Figure 24: The Opened Default Hinge in 200 mM NaCl in Different Concentrations of Thrombin. The distributions either stay the same as the thrombin concentrations increase.

Figure 22 shows that in the 200 mM NaCl, the angular distribution of the Control Hinge stays the same as the thrombin concentration increases. The uniform nature of the probability distribution shows that the Control Hinge is functioning well regardless of how much thrombin is present in solution. Figure 23 shows that the angular distribution of the Closed Default Hinge shifts to the left as the concentration of thrombin increases. The Closed Default Hinge gains an even higher "under 10°" angular distribution with increasing thrombin concentrations. This is defined as a shift to the left, showing that the hinge is working contradictory to what we expect. This could be due to salt screen effects; the aptamer is only 23 base pairs long, so the excess salt warps the intended secondary structure needed for binding. Another possible source for the problem could be due to the breakdown of the tertiary structure of thrombin, causing a deformation of the aptamer binding pocket. Figure 24 shows that the angular distribution of the Opened Default Hinge also stays the same as the concentration of thrombin increases. This shows that this particular configuration is not working because it is not becoming more closed as the concentration of thrombin increases.

The 200 mM NaCl buffer conditions are shown to not be ideal because while it causes the same results in the Control and Opened Default Hinge, it caused the Closed Default Hinge to lose its functionality. This loss of functionality is attributed to the low salt threshold of thrombin. Since thrombin doesn't function well in this high of a salt concentration, it starts to aggregate, which causes low binding affinity problems with the hinge structure. This aggregation is shown in Figure 25 below.

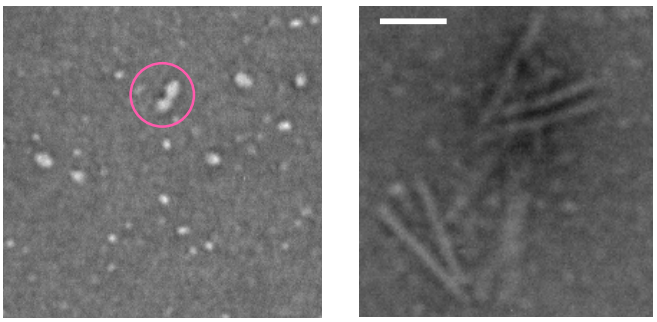

Figure 25: Aggregation of Thrombin and Hinges. In the left image, the pink circle indicates the position of a thrombin aggregate in the 200 mM NaCl solution. In the right images, aggregations of Closed Default Hinges are seen in the presence of thrombin in 200 mM NaCl solution.

The angular distributions led to the conclusion that the 140 mM NaCl solution is the ideal buffer and the Closed Default Hinge is the more optimized protein sensor.

Chapter 4: Conclusions and Future Work

The development of a universal protein sensor is relevant to the treatment of Type 1 diabetes. Current methods of treatment cause numerous complications, and if they are not used properly, they can lead to several other diseases, including neuropathy, nephropathy, and even death. The universal protein sensor would be able to detect the presence of glucose in the blood, allowing for monitoring blood glucose levels without the need for a continuous glucose monitoring system and without drawing multiple blood samples a day to measure blood glucose levels. Novel nanotechnology known as DNA origami can be used to create and optimize this universal protein sensor.

DNA origami allows for the creation of unique structures through the specialized folding of DNA. Using this technique, a hinge structure can be created that contains small DNA strands (aptamers) that have a high affinity and high specificity for thrombin. The hinge structure comes in three configurations. The Control Hinge contains no aptamers and does not interact with thrombin. The Closed Default Hinge contains aptamers that allow it to go from the closed configuration to the open configuration upon contact with thrombin. The Opened Default Hinge goes from open to close when thrombin is present. Between the Closed and the Opened Default, the Closed Default functions better in solution and is actually able to open in the presence of thrombin whereas the Opened Default does not close in the presence of thrombin. A 140 mM NaCl solution and a 200 mM NaCl solution are used to determine the ideal buffer conditions. The 140 mM NaCl is the more ideal buffer because it does not cause the aggregation of thrombin and allows for the thrombin to bind to the aptamers.

Future experiments will go forward with the Closed Default Hinge Structure. The design will be corrected to allow for more opening of the structures in thrombin solution, so that there is

minimal closed structure when thrombin is introduced. One way to improve the structure is to create a complementary strand that has lower affinity for the aptamer. To lower the affinity of the complementary strand, the nucleotide sequence can be changed to contain lesser complementary base pairs. The design will also include a quencher-fluorophore system, such as the one shown in Figure 26.

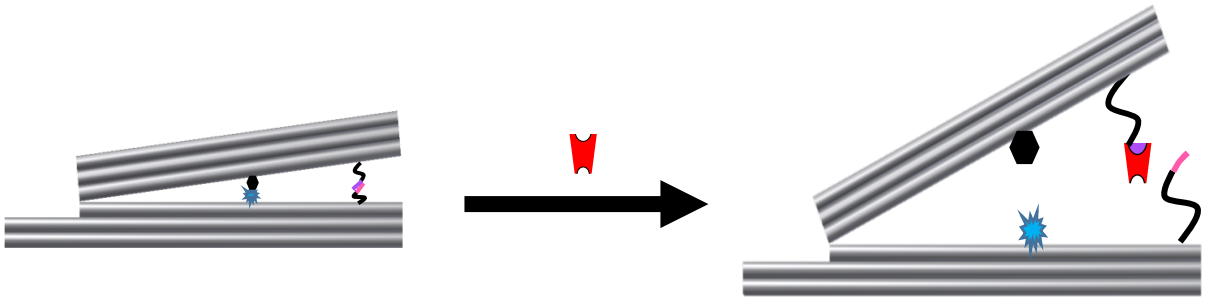

Figure 26: Quencher-Fluorophore system on Closed Default Hinge. The quencher (black hexagon) blocks the emission of the fluorescence (blue) when the hinge is closed and no thrombin (red) is present. When thrombin is introduced and the hinge opens, the quencher moves away from the fluorescence, and the signal fluoresce.

The quencher will quench the fluorescence when there is no thrombin and the hinge is closed. The quencher moves away from the fluorescence when thrombin is present and the observed intensity of the fluorophore molecule increases. A similar measurement approach was previously used to detect conformational changes of a DNA origami mechanism[26]. With the addition of the quencher-fluorophore system, the speed of the hinge opening and closing can be measured in real-time. This allows us to measure the reaction time of the hinge to the presence of thrombin and further characterize functionality.

Ultimately if this universal protein sensor can be functional within live tissue and with the human body, it can replace current methods of blood glucose monitoring. The sensor has less complications associated with it, and it functions more closely to the natural blood glucose

detection system within the body. This can alleviate many of the problems diabetics have and give them a higher quality of life.

Bibliography

[1] Maahs, David M., Nancy A. West, Jean M. Lawrence, and Elizabeth J. Mayer-Davis. "Chapter 1: Epidemiology of Type 1 Diabetes." *Endocrinology and Metabolism Clinics of North America*. U.S. National Library of Medicine, 1 Sept. 2011. Web. 15 Apr. 2016.
[2] "Facts: Type 1 Diabetes." *JDRF*. JDRF, Dec. 2011. Web. 15 Apr. 2016.
[3] "Type 1 Diabetes Mellitus." *Drugs.com*. Harvard Health Publications, n.d. Web. 15 Apr. 2016.
[4] Mayo Clinic Staff. "Type 1 Diabetes." *Treatments and Drugs*. Mayo Clinic, 2 Aug. 2014. Web. 15 Apr. 2016.
[5] "Type 1 Diabetes-Treatment Overview." *WebMD*. WebMD, 29 Sept. 2014. Web. 15 Apr. 2016.
[6] "Brands and Types of Insulin." *WebMD*. WebMD, 4 Dec. 2015. Web. 15 Apr. 2016.
[7] "Insulin Pump." *WebMD*. WebMD, 14 Nov. 2014. Web. 15 Apr. 2016.
[8] O'Donnell, Stacy, and Andrea Penney. "Insulin Injections vs. Insulin Pump." *Joslin Diabetes Center*. Joslin Diabetes Center, n.d. Web. 15 Apr. 2016.
[9] "Insulin Pumps." *American Diabetes Association*. American Diabetes Association, 29 June 2015. Web. 15 Apr. 2016.
[10] Chait, Jan. "Pump Training." *Diabetes Self-Management*. Diabetes Self-Management, 17 Apr. 2013. Web. 15 Apr. 2016.
[11] Olansky, Leann, and Laurence Kennedy. "Finger-Stick Glucose Monitoring: Issues of Accuracy and Specificity." *Diabetes Care* 33.4 (2010): 948–949. *PMC*. Web. 15 Apr. 2016.
[12] "Continuous Glucose Monitoring." *Continuous Glucose Monitoring*. National Institute of Diabetes and Digestive and Kidney Disease, Dec. 2008. Web. 15 Apr. 2016.
[13] Mayo Clinic Staff. "Type 1 Diabetes." *Complications*. Mayo Clinic, 2 Aug. 2014. Web. 15 Apr. 2016.
[14] Nimase, P. Kumar, Vidyasagar Gali, D. M. Suryawanshi, and R. S. Bathe. "Nanotechnology and Diabetes." *International Journal of Advances in Pharmaceutics* 2.13 (2014): n. pag. 2013. Web. 15 Apr. 2016.
[15] George, Alexa. "The Smart Tattoo and Its Potential in Diabetes." University of Pittsburg, n.d. Web. 15 Apr. 2016.
[16] De Prete, Daniel. "Structure of DNA." *Genetics*. N.p., n.d. Web. 15 Apr. 2016.
[17] Seeman, N. "Nucleic Acid Junctions and Lattices." *Journal of Theoretical Biology* 99 (1982):237- 247.
[18] Chen, J., Seeman, N. "Synthesis from DNA of a molecule with the connectivity of a cube." *Nature*. 350 (1991):631-633.
[19] Rothemund, Paul. "Folding DNA to create nanoscale shapes and patterns." *Nature* 440 (2006):297-302.
[20] Halley, P. D., Lucas, C. R., McWilliams, E. M., Webber, M. J., Patton, R. A., Kural, Comert., Lucas, D. M., Byrd, J. C. and Castro, C. E. (2016), DNA Origami: Daunorubicin-Loaded DNA Origami Nanostructures Circumvent Drug-Resistance Mechanisms in a Leukemia Model (Small 3/2016). Small, 12: 307. doi:10.1002/smll.201670014
[21] Douglas, Shawn M., Ido Bachelet, and George M. Church. "A logic-gated nanorobot for targeted transport of molecular payloads." *Science* 335.6070 (2012): 831-834.
[22] "Statistics About Diabetes." *American Diabetes Association*. American Diabetes Association, 1 Apr. 2016. Web. 15 Apr. 2016.

[23] "Why Is Diabetes Research So Important?" *Orlando Clinical Research Center*. Orlando Clinical Research Center, 6 Oct. 2015. Web. 15 Apr. 2016.
[24] Deeb, Larry C. "Diabetes technology during the past 30 years: a lot of changes and mostly for the better." *Diabetes Spectrum* 21.2 (2008): 78.
[25] Halley, P. D., Lucas, C. R., McWilliams, E. M., Webber, M. J., Patton, R. A., Kural, Comert., Lucas, D. M., Byrd, J. C. and Castro, C. E. (2016), DNA Origami: Daunorubicin-Loaded DNA Origami Nanostructures Circumvent Drug-Resistance Mechanisms in a Leukemia Model (Small 3/2016). Small, 12: 307. doi:10.1002/smll.201670014
[26] Marras, Alexander E., Zhou, Lifeng, Sun, Hai-Jun, and Castro, Carlos E. (2015), Programmable motion of DNA origami mechanisms PNAS 2015 112 (3) 713-718; doi:10.1073/pnas.1408869112
[27] "What Is an Aptamer?" *Base Pair Biotechnologies Aptamer Discovery and Research What Is an Aptamer Comments*. Base Pair Biotechnologies Aptamer Discovery and Research What Is an Aptamer Comments, 2016. Web. 15 Apr. 2016.
[28] Cai, Baobin, et al. "Stability and bioactivity of thrombin binding aptamers modified with D-/L-isothymidine in the loop regions." *Organic & biomolecular chemistry* 12.44 (2014): 8866-8876.
[29] Castro, C., Kilchherr, F., Kim, D, Shiao, E., Wauer, T., Wortmann, P., Bathe, M., Dietz, H. "A primer to scaffolded DNA origami." *Nature Methods.* 8(2011):221-229.
[30] Stahl E, Martin TG, Praetorius F, Dietz H. Facile and Scalable Preparation of Pure and Dense DNA Origami Solutions. *Angewandte Chemie (International Ed in English)*. 2014;53(47):12735-12740. doi:10.1002/anie.201405991.